Designing Smac-mimetics as antagonists of XIAP, cIAP1, and cIAP2

Federica Cossu [a], Eloise Mastrangelo [a,b], Mario Milani [a,b], Graziella Sorrentino [a], Daniele Lecis [c], Domenico Delia [c], Leonardo Manzoni [d,e], Pierfausto Seneci [e,f], Carlo Scolastico [e,f], Martino Bolognesi [a,b,*]

[a] *Department of Biomolecular Sciences and Biotechnology, University of Milano, Via Celoria 26, I-20133 Milano, Italy*
[b] *CNR, Istituto Nazionale Fisica della Materia (INFM), Via Celoria 26, I-20133 Milano, Italy*
[c] *Department of Experimental Oncology, Fondazione IRCCS, Istituto Nazionale dei Tumori, Via Venezian 1, I-20133 Milano, Italy*
[d] *CNR, Istituto di Scienze e Tecnologie Molecolari (ISTM), Via Golgi 19, I-20133 Milano, Italy*
[e] *Centro Interdisciplinare Studi bio-molecolari e applicazioni Industriali (CISI), University of Milano, Via Venezian 21, I-20133 Milano, Italy*
[f] *Department of Organic and Industrial Chemistry, University of Milano, Via Venezian 21, I-20133 Milano, Italy*

ARTICLE INFO

ABSTRACT

Inhibitor of apoptosis proteins (IAPs) such as XIAP, cIAP1, and cIAP2 are upregulated in many cancer cells. Several compounds targeting IAPs and inducing cell death in cancer cells have been developed. Some of these are synthesized mimicking the N-terminal tetrapeptide sequence of Smac/DIABLO, the natural endogenous IAPs inhibitor. Starting from such conceptual design, we generated a library of 4-substituted azabicyclo[5.3.0]alkane Smac-mimetics. Here we report the crystal structure of the BIR3 domain from XIAP in complex with Smac037, a compound designed according to structural principles emerging from our previously analyzed XIAP BIR3/Smac-mimetic complexes. In parallel, we present an *in silico* docking analysis of three Smac-mimetics to the BIR3 domain of cIAP1, providing general considerations for the development of high affinity lead compounds targeting three members of the IAP family.

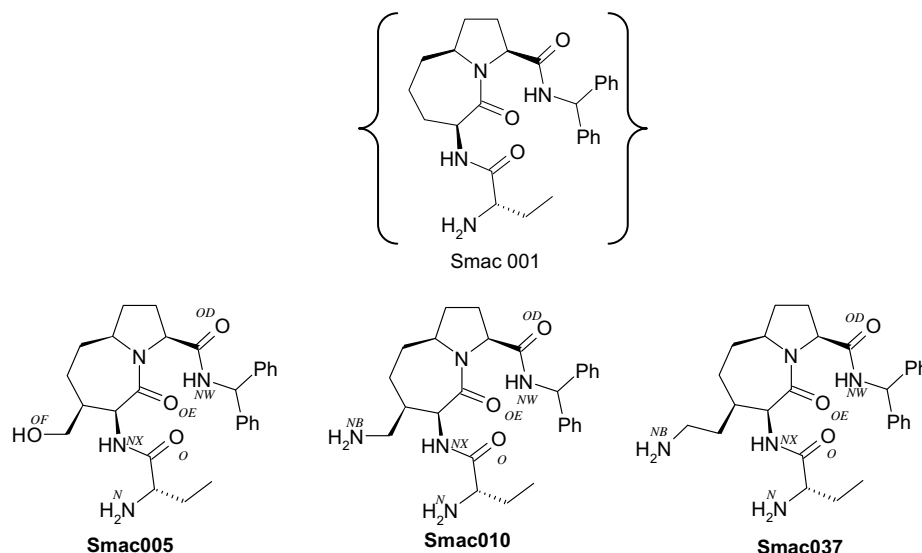© 2008 Elsevier Inc. All rights reserved.

Apoptosis is a cellular process of programmed death essential for homeostasis maintenance in multicellular organisms [1]. Inappropriate apoptotic regulation has been implicated in many human diseases, including cancer [2,3] and neurodegeneration [4]; regulation of the apoptotic pathway has therefore become focus of extensive pharmaceutical research. Apoptosis initiation and execution phases are both dependent on a subset of caspases (cysteine-dependent aspartyl-specific proteases) that are regulated by members of the IAP (Inhibitor of Apoptosis Proteins) family [5,6]. Within the IAP family, XIAP (X-chromosome-linked IAP), cIAP1 and cIAP2 (cellular IAPs) are characterized by three tandem BIR (Baculoviral IAP Repeat) domains (BIR1-3), and by a C-terminal RING domain, endowed with E3 ubiquitin ligase activity. In addition, cIAP1 and cIAP2 host a CAspase Recruitment Domain (CARD) located before the RING domain; cIAP1 and cIAP2 associate with two necrosis factor receptors (TNFR) signaling proteins, TRAF1 and TRAF2, to participate in TNF α-in-duced NF-kB activation [7,8]. In contrast, XIAP inhibits apoptosis by binding to and inhibiting caspase-9 (initiator caspase) through its BIR3 domain [9], and caspase-3 and -7 (executioner caspases) through its BIR2 domain [10,11]. The Second Mitochondria-derived Activator of Caspases (Smac)/Direct IAp Binding with LOw pI (DIABLO) protein [12,13] is an endogenous antagonist of IAPs. High levels of XIAP have been found in several cancer cells lines [14]; in such cases, the physiological amounts of Smac/DIABLO released from the mitochondria may not be sufficient to overcome the inhibitory effect of XIAP on caspases. Inactivation of overexpressed XIAP by Smac-mimetic molecules may relieve caspase inhibition, thereby promoting apoptosis in malignant cells [15–20]. It has been shown that small Smac-mimetic inhibitors, such as Smac001 (Fig. 1) inspired by the Smac N-terminal AVPI sequence [21], can bind the XIAP BIR3 domain with submicromolar potency, promoting apoptosis in tumor cells.

Starting from the structure of Smac001 we generated a library of 4-substituted azabicyclo [5.3.0] alkane lead compounds, which display enhanced affinity to XIAP linker-BIR2 and/or BIR3 domains [22]. Crystal structure analysis of the complexes between XIAP BIR3 and two 4-substituted Smac-mimetics (Smac005 and Smac010, Fig. 1) brought us to the synthesis of Smac037 [22], displaying a longer 4-substituted azabicyclo[5.3.0]alkane arm (-CH$_2$-CH$_2$-NH3$^+$; Fig. 1). Here we report the crystal structure of Smac037 in complex with

Fig. 1. Chemical structures of Smac005, Smac010, and Smac037. For ease of comparison the chemical formulae of the Smac-mimetics dealt with are reported; arbitrary names have been assigned to the atoms involved in main interactions with the BIR3 domain, in the three different compounds. In brackets the chemical structure of Smac001 [21].

XIAP BIR3 solved at 3 Å resolution. Moreover, since Smac-mimetics have been reported to kill cancer cells mainly by inducing the degradation of cIAP1 and cIAP2 [19,20,23], we analyzed through in silico molecular modeling/docking the binding mode of Smac005, Smac010, and Smac037 to the cIAP1 BIR3 domain, whose crystal structure is known [24]. The structure and simulation results are discussed at the light of in vitro experiments showing the effective degradation of cIAP1 induced by the Smac-mimetics proposed here.

Materials and methods

Chemistry, cloning, expression, purification, and crystallization of XIAP BIR3/Smac037. Human XIAP BIR3 domain and Smac037 were produced/purified as described [22,25]. The purified recombinant protein was stored in 20 mM Tris pH 7.5, 200 mM NaCl, 10 mM DTT, and concentrated to 10 mg ml^{-1}. Microbatch crystallization experiments were assembled using an Oryx-8 crystallization robot (Douglas Instruments, East Garston, UK), from a 2:1 mixture of the protein stock solution with 5 mM of Smac037, and the precipitant solution. The 0.3 μl assembled droplets were covered by equal amounts of al's oil and paraffin oil. The crystallization screening solutions were those of Crystal Screens I and II and Index from Hampton Research (Aliso Viejo, CA, USA), Wizard 1 e 2 (deCode Genetics, Emerald Biostructures Products), and of the JBScreening Classic 1, 2, 3, and 4 (Jena Bioscience GmbH, Jena, Germany). Very small crystals, obtained in 0.1 M ammonium acetate, 0.1 M BIS–Tris pH 5.5, 17% PEG 10K, were used for microbatch seeded crystallization experiments, assembled from a 2:1:1 mixture of the protein solution containing 5 mM Smac037, the suspended microseeds, and precipitant solutions, for a total volume of 0.5 μl. Prismatic crystals of approximately $200 \times 30 \times 30 \; \mu m^3$ of the XIAP BIR3/Smac037 complex were obtained after 1 week, at 20 °C, using 0.2 M magnesium formate as precipitant. Before X-ray data collection, crystals were soaked in a cryoprotectant solution (0.2 M magnesium formate, 25% glycerol) and flash-cooled in liquid nitrogen. The crystals diffracted to a maximum resolution of 3.0 Å using synchrotron radiation on beam-line ID 23-1, at the ESRF (Grenoble, France). The diffraction data were processed with MOSFLM [26], and intensities were merged using SCALA [27].

Structure determination and refinement. The three-dimensional structures of XIAP BIR3/Smac037 was solved by the molecular replacement method using the program Phaser (3.0 Å resolution [28]) and the XIAP BIR3 structure in complex with Smac005 (PDB id 3CLX [22]) as search model. The two BIR3/Smac037 independent molecules located by molecular replacement were subjected to rigid-body refinement (R/Rfree = 36.5/38.8), and subsequently refined/modeled using REFMAC5 and Coot [29–31]. Inspection of difference Fourier maps at an intermediate refinement stage showed strong residual density, located between the α3 helix and the main β-sheet, compatible with one Smac-mimetic inhibitor that was accordingly model-built for each molecule in the asymmetric unit.

The refined XIAP BIR3/Smac037 model covers residues 254–354; while the N-terminal residues 241–253 and the last C-terminal residues 355–356 are disordered. The stereochemical quality of

Table 1
Data collection and refinement statistics for BIR3/Smac037.

Data collection statistics	
Space group	I4$_1$32
	$a = b = c = 170.4$ Å
Unit-cell parameters	$\alpha = \beta = \gamma = 90°$
Solvent content%	64.2
No. of molecules per asymmetric unit	2
Resolution (Å)	40.0–3.0
Mosaicity (°)	0.7
No. of unique reflections	8730 (1243)
Completeness (%)	99.7 (100)
Redundancy	11.6 (12.0)
R_{merge}[a] (%)	9.2 (66.3)
Average I/σ (I)	20.9 (3.7)
Refinement statistics	
R_{factor}[b] (%)	18.9
R_{free}[c] (%)	23.9
r.m.s. bond lengths (Å)	0.007
r.m.s. bond angles (°)	1.06
Average protein B factor (Å^2)	50.6
Ramachandran plot	
Residues in most favoured regions (%)	87.1%
Residues in additionally allowed regions (%)	12.9%

Values in parentheses are for the highest resolution shell: 3.16–3.00 Å.
  [a] $R_{merge} = \Sigma \; |I - (I)|/\Sigma \; I \times 100$, where I is intensity of a reflection and (I) is its average intensity.
  [b] $R_{factor} = \Sigma \; |F_o - F_c|/\Sigma|F_o| \times 100$.
  [c] R_{free} is calculated on 5% randomly selected reflections, for cross-validation.

the model [32] together with data collection and refinement statistics are summarized in Table 1. Atomic coordinates and structure factors for XIAP BIR3/Smac037 complex have been deposited with the Protein Data Bank [33] with accession code 3EYL.

Molecular modeling of Smac-mimetics cIAP1 interaction. Auto-Dock4 [34] was used for the docking analysis and Python Molecule Viewer 1.4.5 (http://mgltools.scripps.edu/packages/pmv) to analyze the data. The cIAP1 BIR3/SmacAVPIAQ structure (PDB id 3D9U [24]) was used to model the binding of Smac005, Smac010 and Smac037 to the cIAP1 BIR3 domain. The center of the docking search was set at Leu313, with a search grid extending 52 grid points in each dimension (148877 grid nodes, with a period of 0.375 Å) resulting in a cubic box of 20 Å/edge. In the docking simulation the protein was constrained as a rigid body while the Smac-mimetic molecules were allowed free rotation around all single bonds (11 rotatable bonds for Smac005, 12 for Smac010, and 13 for Smac037, respectively). Fifty independent genetic algorithm (GA) runs were used to carry over the docking procedure [34]. The conformations showing lower free energy of binding for each ligand were saved for analysis of the docking models.
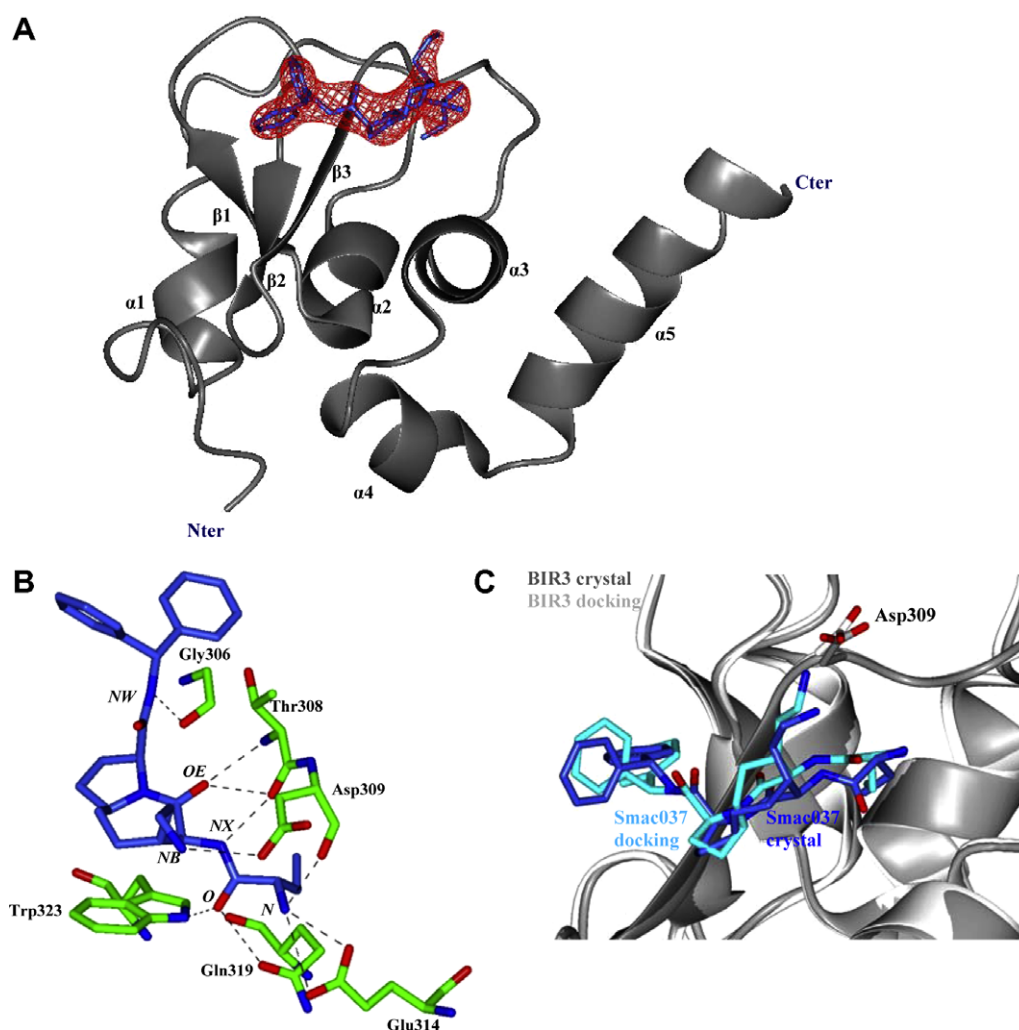
IAP degradation cell-based assays. The MDA-MB231 cell line was treated with 5 μM of each Smac-mimetic, or left untreated as control. After 3 h, cells were harvested and lysed. Proteins were revealed by Western blot using antibodies specific for XIAP (BD Biosciences), cIAP1 (R&DSystems), and βActin (Sigma) as control.

Results and discussion

Crystal structures of XIAP BIR3/Smac037 complex

The XIAP BIR3/Smac037 complex crystallized in the cubic space group I4$_1$32, with unit cell parameters $a = b = c = 170.4$ Å, two protein molecules in the asymmetric unit ($V_M = 3.4$ Å^3 Da^{-1}, 64.2% solvent content [35]). The protein structure was solved using the molecular replacement method, and refined to 3.0 Å resolution, to R/Rfree values of 18.9/23.9% (Table 1).

As previously reported [36], the XIAP BIR3 domain is composed of five α-helices (α 1–2 at the N terminus, and α 3–5 at the C-terminus), and a three-stranded β-sheet, hosting a Zinc-finger motif. The α5 helix of the XIAP BIR3/Smac037 complex here reported is

Fig. 2. (A) Overall architecture of XIAP BIR3 domain (in white) showing the five α-helices and the three anti-parallel β-strands. The red cage shows the Fo–Fc difference Fourier map (contoured at 3σ), calculated after few refinement cycles of the protein structure alone. The difference electron density falls in the IBM groove, comprised between the β3 strand and the α3 helix, where Smac037 has been modeled (in light blue). (B) BIR3/Smac037 interaction network. The main residues involved in stabilizing interactions are shown. Smac037 is in light blue, while the protein residues (labeled) are green; nitrogen atoms are shown in blue, oxygen in red; the main hydrogen bonds linking BIR3 and Smac037 are shown as dashed lines. (C) Superposition of the XIAP BIR3/Smac037 docked model (showing the lowest free energy of binding) on the XIAP BIR3/Smac037 crystal structure. The XIAP BIR3 protein component crystal structure and residue Asp309 are in grey, the docked model is in white. The Smac037 molecule of the crystal structure is light blue, the docked molecule is cyan. (For interpretation of the references to color in this figure legend, the reader is referred to the web version of this article.)

involved in intermolecular contacts, resulting in a dimeric BIR3 assembly, stabilized in the crystal asymmetric unit by a Cys351-Cys351′ disulfide bridge (buried area 890 Å², as defined by program PISA; http://www.ebi.ac.uk/msd-srv/prot_int/pistart.html). Both asymmetric unit BIR3 chains showed strong residual electron density, located in the IAP binding motif (IBM) groove, comprised between the β3 strand and the α3 helix, that could be modeled and refined as a bound Smac037 moiety (Fig. 2A).

The XIAP BIR3/Smac037 complex in comparison with XIAP BIR3/Smac005 and BIR3/Smac010 crystal structures

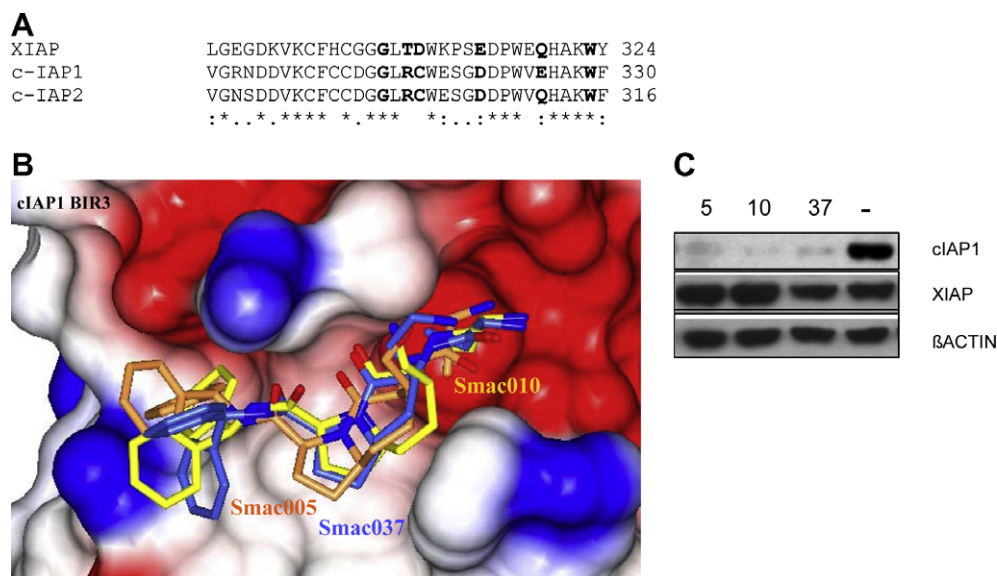We designed Smac037 elongating the grafted arm of Smac010 by a methylene group [22] in order to (i) establish an electrostatic interaction with Asp309 (as in Smac010), and (ii) avoid a previously observed shift of the inhibitor moiety in the IBM (as in Smac010 [22]). The crystal structure of the XIAP-BIR3/Smac037 complex shows that all the protein/inhibitor interactions displayed by Smac005 are preserved in Smac037 and, in addition, a new electrostatic interaction between the elongated 4-substituted azabicyclo [5.3.0] alkane arm and Asp309 is established.

As described for other XIAP inhibitors, binding of Smac037 to the BIR3 IBM groove is stabilized by a network of hydrogen bonds and van der Waals contacts involving Gly306, Thr308, and Asp309, in the β3 strand, and Glu314, in the β3–α3 loop (Fig. 2B). Details of the XIAP BIR3/Smac037 stabilizing interactions are summarized in Table 2, in comparison to XIAP BIR3/Smac005 and Smac010 interactions previously reported [22]. From the analysis of such data we

Table 2
Summary of the interaction network stabilizing the XIAP BIR3/Smac037 complex. In parentheses the average interatomic distances of the three XIAP BIR3/Smac037 models generated by the docking analysis [22]. The average distances observed in XIAP BIR3 complexes with Smac005 and Smac010 [22] are reported in the fourth column for comparison. cIAP1 residues structurally matching those of XIAP BIR3 domain together with the ligand/protein interactions predicted by in silico docking are reported in the last three columns.

XIAP BIR3	Interaction	Smac037 crystal (docking)	Smac005/Smac010	cIAP1 BIR3	Interaction	Smac005/Smac010/Smac037
Gly306	O-NW	3.3 (2.8)	3.3/3.7	Gly312	O-NW	3.3/3.8/4.0
Thr308	N-OE	2.8 (3.0)	3.1/2.9	Arg314	N-OE	2.7/3.4/2.8
	O-NX	3.2 (2.7)	3.0/2.8		O-NX	2.8/NA/3.0
					N-NX	2.8/NA/NA
					Nε-OD	3.1/NA/NA
Asp309	O-N	3.2 (3.1)	3.3/3.4	Cys315	O-N	3.4/NA/NA
	Oδ-NB	3.6 (3.4)	-/3.3		O-NB	-/2.7/NA
Glu314	Oε1-N	2.9 (2.8)	2.8/2.8	Asp320	Oδ1-N	NA/NA/3.5
	Oε2-N	3.0 (2.9)	3.0/2.9		Oδ2-N	2.9/NA/2.8
					Oδ1-NB	-/3.9/NA
					Oδ2-NB	-/2.6/NA
Gln319	Oε1-O	3.8 (3.6)	3.3/NA	Glu325	Oε1-O	3.2/NA/3.1
					Oε1-N	3.8/2.8/2.7
					Oε2-N	NA/2.6/NA
					Oε2-NX	NA/2.8/NA
Trp323	Nε1-O	3.3 (3.4)	3.2/NA	Trp329	Nε1-O	3.3/NA/NA

Fig. 3. (A) Structure-based alignment of the XIAP and cIAP1 and cIAP2 BIR3 amino acids mainly building the IBM groove. In bold the amino acids involved in the interaction network. (B) Superposition of the cIAP1 BIR3/Smac005 /Smac010 and /Smac037 simulated complex models. Smac037 (from the crystal structure) is light blue, Smac005 is coral and Smac010 is yellow. The color coded cIAP BIR3 molecular surface (electrostatic potential coding: red -39 kTe⁻¹, blue +39 kTe⁻¹) shows matching of the polar/apolar components of the Smac-mimetics molecules with the surface properties of the BIR3 domain. (C) cIAPs degradation in presence of Smac005, Smac010 and Smac037. The blot was normalized for the levels of β-Actin. The symbol − refers to untreated cells. (For interpretation of the references to color in this figure legend, the reader is referred to the web version of this article.)

can conclude that XIAP BIR3/Smac037 crystal structure displays most of the interactions predicted by our previous docking model [22], within ±0.2 Å of the intermolecular contacts length observed (Table 2 and Fig. 2C). As a result, the overall agreement between the crystal structure here presented and the theoretical docking model of the XIAP BIR3/Smac037 complex previously reported [22] prompted us to investigate the cIAP1/Smac-mimetics interaction using *in silico* docking approaches (see below).

Smac-mimetics role in cIAPs inhibition

It has recently been reported that Smac-mimetics can kill malignant cells by binding to cIAP1 and cIAP2, leading to TNF-receptor mediated apoptosis [19,20,23]. The three members of the IAP family, XIAP, cIAP1, and cIAP2, are structurally homologous (XIAP amino acid sequence identity to cIAP1 and cIAP2 of 36% and 39%, respectively, the amino acid sequence identity between cIAP1 and cIAP2 is 70%). In particular, the BIR3 IBM region, where the critical residues involved in Smac-mimetics recognition are located, is well conserved among the three IAPs (Fig. 3A). The XIAP BIR3 residues involved in van der Waals contacts (Val298, Lys299, and Trp310) and hydrogen bonds (Gly306, Leu307, and Trp323) with the inhibitory compounds are conserved (Fig. 3A). Minor exceptions are Leu292, replaced by Val in the cIAPs, Glu314 substituted by Asp in both cIAPs, and Gln319, which is Glu325 in cIAP1, and Gln311 in cIAP2. Finally, residues Thr308 and Asp309 that were found relevant for Smac-mimetics interaction with XIAP BIR3, are replaced by Arg314/Arg300 and Cys315/Cys307 in cIAP1/cIAP2, respectively (Fig. 3A).

Based on the above observations we speculated that the Smac-mimetics here discussed could also bind to, and inhibit, the cIAP BIR3 domains. To further investigate such hypothesis, we performed Smac-mimetics docking simulations on the recently published structure of cIAP1 BIR3 (PDB id 3D9U [36]). The docked models produced show that essentially the same set of Smac-mimetic/XIAP BIR3 interactions described above can be established to the cIAP1 BIR3 domain (Fig. 3B and Table 2). Among these, the crucial hydrogen bonds with the backbone of the conserved Gly312 (corresponding to XIAP Gly306), and with Arg314 (XIAP Thr308). cIAP1 Asp320 and Glu325 side chains may interact with the N-terminal portion of the Smac-mimetics, similarly to Glu314 and Gln319 in XIAP BIR3. On the other hand, loss of Smac-mimetic interaction with Cys315 (XIAP Asp309) and Trp329 (XIAP Trp323) may be balanced in cIAP1 BIR3 by the gain of multiple hydrogen bonds to Glu325 (Gln319 in XIAP BIR3), to Glu319 (XIAP Lys311), and to the backbone of Leu313.

Since the interactions of the Smac-mimetics with cIAP1 BIR3 predicted by the docking algorithms suggested efficient binding, which may result in promoting cIAP1 auto ubiquitination and receptor-mediated apoptosis [19,20,23], we tested *in vitro* the effects of Smac005, Smac010 and Smac037 in inducing cIAPs degradation in the MDA-MB231 cell line. The results of such tests, as indicated by Western blot analysis, show that all three Smac-mimetics effectively induce cIAP1 degradation (Fig. 3C).

Conclusions

The structure-based analysis of Smac005 and Smac010 recognition by the XIAP BIR3 domain led us to design Smac037. The XIAP BIR3/Smac037 crystal structure, in agreement with our previous *in silico* studies (Fig. 2C, [22]), confirms the validity of the design criteria adopted. Moreover, we have shown that the three Smac-mimetics considered are effective in inducing cIAPs degradation, an experimental observation that is in keeping with their (simulated) binding to cIAP1 BIR3 domain. These results, together with

consideration of the Smac-mimetic/BIR3 domain recognition principles detailed, cast new ideas for the development of lead compounds able to bind XIAP, cIAP1 and cIAP2, thus targeting different aspects of the apoptotic pathway.

References

[1] H. Steller, Mechanism and genes of cellular suicide, Science 267 (1995) 1445–1449.
[2] S. Fulda, K.M. Debatin, Targeting apoptosis pathways in cancer therapy, Curr. Cancer Drug Targets 4 (2004) 569–576.
[3] R. Kim, Recent advances in understanding the cell death pathways activated by anticancer therapy, Cancer 103 (2005) 1551–1560.
[4] M. Okouchi, O. Ekshyyan, M. Maracine, T.Y. Aw, Neuronal apoptosis in neurodegeneration, Antioxid. Redox Signal. 9 (2007) 1059–1096.
[5] Q.L. Deveraux, T.C. Reed, IAP family proteins: suppressors of apoptosis, Gene Dev. 13 (1999) 239–252.
[6] E.C. La Casse, S. Baird, R.G. Korneluk, A.E. MacKenzie, The inhibitors of apoptosis (IAPs) and their emerging role in cancer, Oncogene 17 (1998) 3247–3259.
[7] M. Rothe, M.G. Pan, W.J. Henzel, T.M. Ayres, D.V. Goeddel, The TNFR2-TRAF signaling complex contains two novel proteins related to baculoviral inhibitor of apoptosis proteins, Cell 83 (1995) 1243–1252.
[8] R.W. Johnstone, A.J. Frew, M.J. Smyth, The TRAIL apoptotic pathway in cancer onset, progression and therapy, Nature Rev. Cancer 8 (2008) 782–798.
[9] E.N. Shiozaki, J. Chai, D.J. Rigotti, S.J. Riedl, P. Li, S.M. Srinivasula, E.S. Alnemri, R. Fairman, Y. Shi, Mechanism of XIAP-mediated inhibition of Caspase-9, Mol. Cell 11 (2003) 519–527.
[10] S.J. Riedl, M. Renatus, R. Schwarzenbacher, Q. Zhou, C. Sun, S.W. Fesik, R.C. Liddington, G.S. Salvesen, Structural basis for the inhibition of caspase-3 by XIAP, Cell 104 (2001) 791–800.
[11] Y. Huang, Y.C. Park, R.L. Rich, D. Segal, D.G. Myszka, H. Wu, Structural basis of caspase inhibition by XIAP: differential roles of the linker versus the BIR domain, Cell 104 (2001) 781–790.
[12] C. Du, M. Fang, Y. Li, L. Li, X. Wang, Smac, a mitochondrial protein that promotes cytochrome *c*-dependent caspase activation by eliminating IAP inhibition, Cell 102 (2000) 33–42.
[13] A.M. Verhagen, P.G. Ekert, M. Pakusch, J. Silke, L.M. Connolly, G.E. Reid, R.L. Moritz, R.J. Simpson, D.L. Vaux, Identification of DIABLO, a mammalian protein that promotes apoptosis by binding to and antagonizing IAP proteins, Cell 102 (2000) 43–53.
[14] B. Vischioni, P. Van der Valk, W.S. Span, F.A.E. Kruyt, J.A. Rodriguez, G. Giaccone, Expression and localization of inhibitor of apoptosis proteins in normal human tissues, Human Pathol. 37 (2006) 78–86.
[15] T.K. Oost, C.H. Sun, R.C. Armstrong, A.S. Al-Assaad, S.F. Betz, T.L. Deckwerth, H. Ding, S.W. Elmore, E.T. Olejniczak, A. Oleksijew, T. Oltersdorf, S.H. Rosenberg, A.R. Shoemaker, K.J. Tomaselli, H. Zou, S.W. Fesik, Discovery of potent antagonists of the antiapoptotic protein XIAP for the treatment of cancer, J. Med. Chem. 47 (2004) 4417–4426.
[16] L. Li, R.M. Thomas, H. Suzuki, J.K. De Brabander, X. Wang, P.G. Harran, A small molecule Smac mimic potentiates TRAIL- and TNFalpha-mediated cell death, Science 305 (2004) 1471–1474.
[17] H. Sun, Z. Nikolovska-Coleska, C.Y. Yang, L. Xu, M. Liu, Y. Tomita, H. Pan, Y. Yoshioka, K. Krajewski, P.P. Roller, S. Wang, Structure-based design of potent, conformationally constrained Smac-mimetics, J. Am. Chem. Soc. 126 (2004) 16686–16687.
[18] K. Zobel, L. Wang, E. Varfolomeev, M.C. Franklin, L.O. Elliott, H.J.A. Wallweber, D.C. Okawa, J.A. Flygare, D. Vucic, W.J. Fairbrother, K. Deshayes, Design, synthesis, and biological activity of a potent Smac-mimetic that sensitizes cancer cells to apoptosis by antagonizing IAPs, ACS Chem. Biol. 1 (2006) 525–533.
[19] J.E. Vince, W.W. Wong, N. Khan, R. Feltham, D. Chau, A.U. Ahmed, C.A. Benetatos, S.K. Chunduru, S.M. Condon, M. McKinlay, R. Brink, M. Leverkus, V. Tergaonkar, P. Schneider, B.A. Callus, F. Koentgen, D.L. Vaux, J. Silke, IAP antagonists target cIAP1 to induce TNF-dependent apoptosis, Cell 131 (2007) 682–693.
[20] E. Varfolomeev, J.W. Blankenship, S.M. Wayson, A.V. Fedorova, N. Kayagaki, P. Garg, K. Zobel, J.N. Dynek, L.O. Elliott, H.J. Wallweber, J.A. Flygare, W.J. Fairbrother, K. Deshayes, V.M. Dixit, D. Vucic, IAP antagonists induce autoubiquitination of c-IAPs, NF-kappaB activation, and TNFalpha-dependent apoptosis, Cell 131 (2007) 669–681.
[21] Z. Nikolovska-Coleska, R. Wang, X. Fang, H. Pan, Y. Tomita, P. Li, P.P. Roller, K. Krajewski, N.G. Saito, J.A. Stuckey, S. Wang, Development and optimization of a

binding assay for the XIAP BIR3 domain using fluorescence polarization, Anal. Biochem. 332 (2004) 261–273.

[22] E. Mastrangelo, F. Cossu, M. Milani, G. Sorrentino, D. Lecis, D. Delia, L. Manzoni, C. Drago, P. Seneci, C. Scolastico, V. Rizzo, M. Bolognesi, Targeting the X-linked inhibitor of apoptosis protein (XIAP) through 4-substituted azabicyclo[5.3.0]alkane Smac-mimetics. Strucuture, activity and recognition principles, J. Mol. Biol., in press, doi:10.1016/j.jmb.2008.09.064.

[23] S.L. Petersen, L. Wang, A. Yalcin-Chin, L. Li, M. Peyton, J. Minna, P. Harran, X. Wang, Autocrine TNFα signaling renders human cancer cells susceptible to Smac-mimetic-induced apoptosis, Cancer Cell 12 (2007) 445–456.

[24] R. Kulathila, B. Vash, D. Sage, S. Cornell-Kennon, K. Wright, J. Koehn, T. Stams, K. Clark, A. Price, The crystal structure of the BIR3 domain from CIAP1 in complex with the N-terminal peptides of SMAC and Caspase-9, in press.

[25] L. Manzoni, D. Arosio, L. Belvisi, A. Bracci, M. Colombo, D. Invernizzi, C. Scolastico, Functionalized azabicycloalkane amino acids by nitrone 1,3-dipolar intramolecular cycloaddition, J. Org. Chem. 70 (2005) 4124–4132.

[26] I. Steller, R. Bolotovsky, M.G. Rossmann, An algorithm for automatic indexing of oscillation images using Fourier analysis, J. Appl. Cryst. 30 (1997) 1036–1040.

[27] P.R. Evans, Data reduction, in: Proceedings of CCP4 Study Weekend on Data Collection and Processing, 1993, pp. 114–122.

[28] A.J. McCoy, R.W. Grosse-Kunstleve, P.D. Adams, M.D. Winn, L.C. Storoni, R.J. Read, Phaser crystallographic software, J. Appl. Cryst. 40 (2007) 658–674.

[29] M.D. Winn, M.N. Isupov, G.N. Murshudov, Use of TLS parameters to model anisotropic displacements in macromolecular refinement, Acta Cryst. D57 (2001) 122–133.

[30] P. Emsley, K. Cowtan, Coot: model-building tools for molecular graphics, Acta Cryst. D60 (2004) 2126–2132.

[31] G.N. Murshudov, A.A. Vagin, E.J. Dodson, Refinement of macromolecular structures by the maximum-likelihood method, Acta Cryst. D53 (1997) 240–255.

[32] R.A. Laskowski, M.W. MacArthur, D.S. Moss, J.M. Thornton, PROCHECK: a program to check the stereochemical quality of protein structures, J. Appl. Cryst. 26 (1993) 283–291.

[33] H.M. Berman, J. Westbrook, Z. Feng, G. Gilliland, T.N. Bhat, H. Weissig, I.N. Shindyalov, P.E. Bourne, The protein data bank, Nucleic Acids Res. 28 (2000) 235–242.

[34] G.M. Morris, D.S. Goodsell, R.S. Halliday, R. Huey, W.E. Hart, R.K. Belew, A.J. Olson, Automated docking using a Lamarckian genetic algorithm and an empirical binding free energy function, J. Comp. Chem. 19 (1998) 1639–1662.

[35] B.W. Matthews, Solvent content of protein crystals, J. Mol. Biol. 33 (1968) 491–497.

[36] G. Wu, J. Chai, T.L. Suber, J.W. Wu, C. Du, X. Wang, Y. Shi, Structural basis of IAP recognition by Smac/DIABLO, Nature 408 (2000) 1008–1012.